ELSEVIER

Thermochimica Acta 307 (1997) 45–50

thermochimica acta

TG–FTIR, DSC and ESCA characterization of histamine complexes with transition metal ions

S. Materazzi*, R. Curini, A. Gentili, G. D'Ascenzo

Dept. of Chemistry, University "La Sapienza", p.le A. Moro, 5-00185, Rome, Italy

Received 3 February 1997; accepted 19 June 1997

Abstract

The thermoanalytical study of some $MeHm_x$ complexes (Hm = histamine; $x = 1, 2$) and $MeHm_x(NO_3)_2$ ($x = 2, 4$) with $Co^{(II)}$, $Ni^{(II)}$ and $Cu^{(II)}$ is reported. By TG–FTIR coupled analysis, the decomposition steps are analyzed and the intermediate reactions are proposed. Results of ESCA analysis for all $Ni^{(II)}$ compounds indicate correct atomic ratios between organic and inorganic nitrogen and are useful for determining metal coordination states. © 1997 Elsevier Science B.V.

Keywords: Complexes; DSC; ESCA; Histamine; TG–FTIR

1. Introduction

Histamine is a small-molecule hormone commonly present in the tissues of living organisms. The contribution of histamine in many physiological and pathological processes, e.g. the regulation of microcirculation and blood pressure, the stimulation of gastric secretion, the mediation of symptoms of allergy and inflammation, etc. and the use in pharmacology, makes it an attractive field for biochemical researchers.

In humans and animals, the main source of histamine is from mast cells, which can capture histamine from the organism, produce and store it, and finally release it. In histamine and anti-histamine activity, an important role is played by transition metal ions such as $Co^{(II)}$, $Cu^{(II)}$ and specially $Ni^{(II)}$ in the formation of metal complexes. In fact, the anti-histamine activity of certain compounds depends upon their competition with histamine for binding receptor sites, which in some cases were shown to be metal ions [1,2].

A variety of data is available in the literature on $Co^{(II)}$, $Ni^{(II)}$ and $Cu^{(II)}$ histamine complexes in aqueous solutions [3–11] and also in the solid state [7,12–18], for some complexes, the crystalline and molecular structure was determined [19,20]. However, not sufficient thermoanalytical data are reported for the determination of an unambiguous decomposition mechanism.

In this work, the thermoanalytical behaviour of MeHm, $MeHm_2$, $MeHm_2(NO_3)_2$ and $MeHm_4(NO_3)_2$ complexes, where Me = $Co^{(II)}$, $Ni^{(II)}$ or $Cu^{(II)}$, has been investigated by DSC and TG–FTIR coupled analysis in order to evaluate thermal stability and, by analysis of the evolved gases [21–23], decomposition steps. Moreover, an ESCA analysis is reported aiming to identify the stoichiometry and coordination state of $Ni^{(II)}$ complexes.

*Corresponding author.

PII S0040-6031(97)00306-7

2. Experimental

2.1. Synthesis of the complexes

Histamine and metal nitrates were obtained from Aldrich. The complexes of general formula $MeHm_x(NO_3)_2$ ($x = 2$, 4) were obtained by mixing the ligand solution (10^{-3} M in absolute ethanol) with the metal solution (10^{-3} M in absolute ethanol) in stoichiometric ratio. The final solution was left at room temperature until precipitate was formed. Under these conditions, only the $MeHm_4(NO_3)_2$ complex was obtained for $Ni^{(II)}$ and all attempts to synthetize the 1 : 4 complexes of $Co^{(II)}$ and $Cu^{(II)}$ failed even when the ligand concentration was increased up to 20 : 1.

The $MeHm_2$ complexes were obtained in aqueous solutions; the 10^{-3} M ligand solution was added to the 10^{-3} M metal solution at pH = pK_{a1} . If the complex did not precipitate, a 1 : 1 ethanol/ethyl ether solution was added stepwise to obtain an oil and then the precipitate. Only for $Co^{(II)}$ the MeHm complex was obtained.

2.2. Instrumental

The thermoanalytical curves were obtained using a Perkin–Elmer TGA7 thermobalance for low temperatures (range 20–1000°C) and a Perkin–Elmer DSC7. The flow atmosphere was argon, nitrogen or air, with a flow rate of 50–100 ml min^{-1}. The heating rate was ranged between 5 and 40°C min^{-1}. The thermobalance was coupled with a Perkin–Elmer FTIR, model 1760X, in order to measure the IR spectra of evolved gases during the thermogravimetric analysis. The TGA7 is coupled to the heated gas cell of the FTIR instrument by means of a heated transfer line. Gaseous or vaporised components are flushed by the suitable gas and the temperatures of the cell and of the transfer line are independently selected. The only materials in contact with the sample gases are PTFE of the transfer line, KBr of the cell windows and the glass of the TGA/7 furnace.

The ESCA spectra were obtained from dry powder samples in a VG ESCALAB MK II spectrometer, equipped with an Al anode X-ray source, an hemispherical analyser and a five channeltron detector. High-resolution spectra were obtained on the energy regions of interest, namely, Ni 2*p*, N 1*s* and C 1*s*. Peak positions and stoichiometries were measured by integrating the peak areas and correcting for the elemental sensitivity factors [24]. Photoemission induced electrostatic charging of the samples was corrected by using the value of 285.0 eV for C 1*s* from hydrocarbons.

3. Results and discussion

3.1. Thermal analysis

The TG and DTG curves of $MeHm_2(NO_3)_2$ complexes (Fig. 1) show two main decomposition steps. As can be seen from Fig. 2, the first TG process is not influenced by the operational atmosphere and the curves in air and nitrogen atmosphere are different only for the second process to give MeO.

The DSC curves (Fig. 3) show two main exothermic processes in the range 220–350°C, the first one is

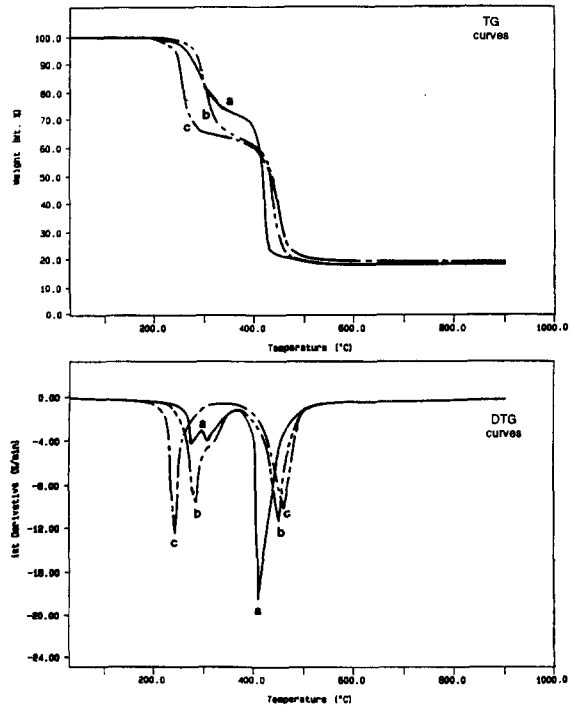

Fig. 1. TG and DTG curves of $MeHm_2(NO_3)_2$ complexes: (a) $Co^{(II)}$ complex, (b) $Ni^{(II)}$ complex, (c) $Cu^{(II)}$ complex. Scanning rate: 10°C min^{-1}, flow rate: air at 50–100 ml min^{-1}.

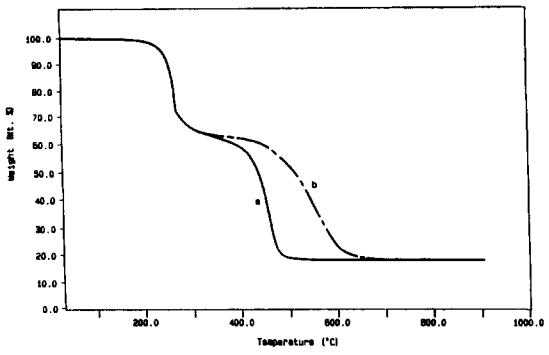

Fig. 2. TG curves of $MeHm_2(NO_3)_2$ complexes: operational atmosphere influence with: (a) air, (b) nitrogen. Scanning rate: 10°C min^{-1}, flow rate: 50–100 ml min^{-1}.

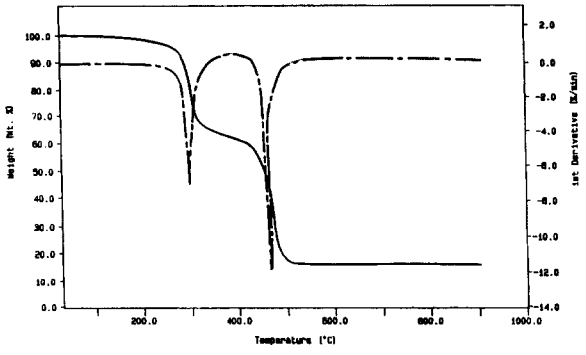

Fig. 4. $NiHm_4(NO_3)_2$ complex:——— TG curve, — — — DTG curve. Scanning rate: 10°C min^{-1}, flow rate: air at 50–100 ml min^{-1}.

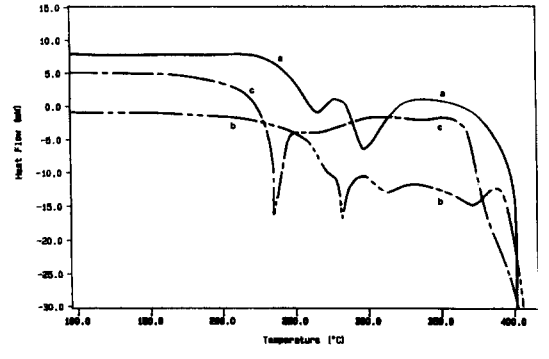

Fig. 3. DSC curves of $MeHm_2(NO_3)_2$ complexes: (a) $Co^{(II)}$ complex, (b) $Ni^{(II)}$ complex, (c) $Cu^{(II)}$ complex. Scanning rate: 10°C min^{-1}, flow rate: air at 50–100 ml min^{-1}.

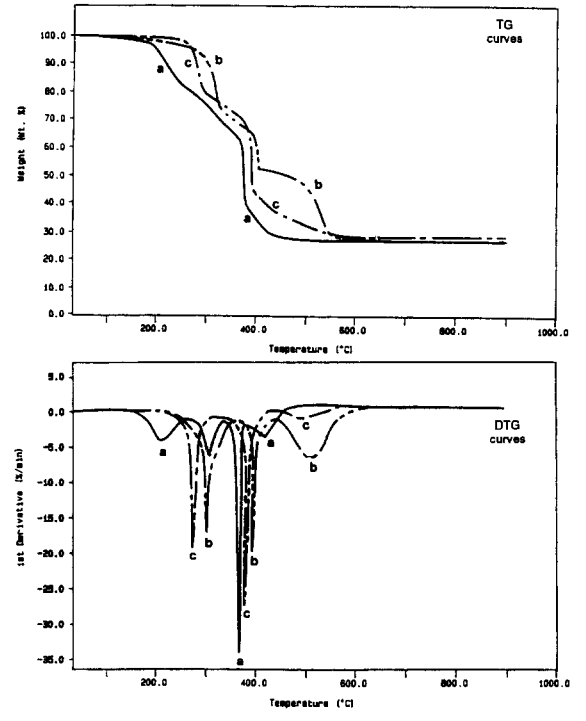

Fig. 5. TG and DTG curves of $MeHm_2$ complexes: (a) $Co^{(II)}$ complex, (b) $Ni^{(II)}$ complex, (c) $Cu^{(II)}$ complex. Scanning rate: 10°C min^{-1}, flow rate: air at 50–100 ml min^{-1}.

sharper for Ni and Cu complexes. Around 360°C all complexes start to decompose with an exothermic peak to give MeO.

The decomposition of $NiHm_4(NO_3)_2$ (Fig. 4) occurs in two well-defined steps to give NiO, and the first of them is not influenced by the atmosphere as for the $NiHm_2(NO_3)_2$ complex.

The DSC curve shows one exothermic peak followed by the exothermic peak of the decomposition.

The thermal decomposition of $MeHm_2$ complexes to MeO occurs in three main TG steps (Fig. 5), from the DSC curves (Fig. 6) the different behaviour of the three complexes in the range 200–350°C can be noted: $NiHm_2$ shows an exothermic process at around 290°C and another exothermic process before the decomposition; $CuHm_2$ has only one exothermic peak shifted to a lower temperature, followed by the decomposition to metal oxide; the $CoHm_2$ complex shows two exothermic processes as for the $Ni^{(II)}$ case, although the first one appears at a lower temperature than the $Cu^{(II)}$ and the $Ni^{(II)}$ complexes before the exothermic decompo-

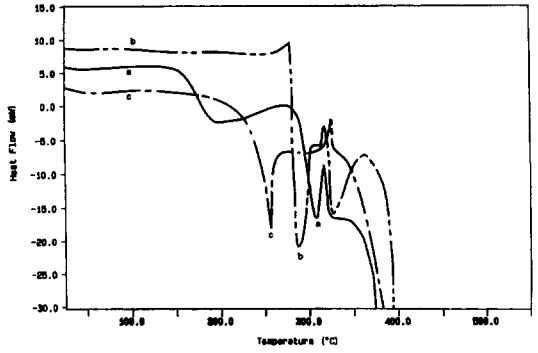

Fig. 6. DSC curves of $MeHm_2$ complexes: (a) $Co^{(II)}$ complex, (b) $Ni^{(II)}$ complex, (c) $Cu^{(II)}$ complex. Scanning rate: 10°C min^{-1}, flow rate: air at 50–100 ml min^{-1}.

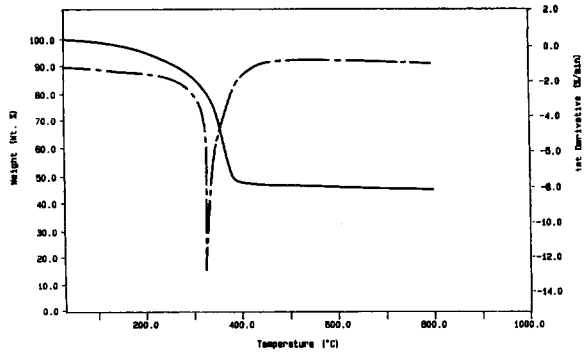

Fig. 7. CoHm complex: ———TG curve,— — — DTG curve. Scanning rate: 10°C min^{-1}, flow rate: air at 50–100 ml min^{-1}.

sition. Around 320°C, all DSC curves show the tendency to return to the base line value. From the observation of both TG and DSC curves of these complexes, the higher thermal stability is shown by $NiHm_2$, followed by $CuHm_2$ and then $CoHm_2$.

Only $Co^{(II)}$ forms the MeHm complex. Its thermal behaviour shows only one decay step to the oxide (Fig. 7). This was also reported by Felix [25]. In his work, Felix explains the 1 : 1 complex by a hydrogen bond which is formed by histamine; the proton release may be a slow LH^+ $L + H^+$ process, and a higher value of the rate constant for the proton release is expected because the cobalt ion destroys the intramolecular hydrogen bond. The thermal decomposition to give CoO falls in the interval 200–385°C and its thermal stability is lower than the $CoHm_2$ complex.

Histamine contains three functional groups which are potential sites for coordinating with metal ions. These are:

- the α-amino group
- the secondary imidazole nitrogen
- the tertiary imidazole ring

As for the imidazole and its substitutes, in non aqueous solvent, the coordination sites are the pyrrolic nitrogen and the amino nitrogen [26–28].

The thermal behaviour of $MeHm_2(NO_3)_2$ complexes, as can be seen from the TG curves, suggests a thermal stability scale for the first process with Ni ≅ Co > Cu, while for the second process Cu ≅ Ni > Co.

3.2. TG–FTIR

The FTIR spectrum of the evolved gas from the $MeHm_2(NO_3)_2$ complexes (Fig. 8) shows, for the first process, bands at 2236–2212 and 1317–1277 cm^{-1} which can be attributed to N_2O release, and bands at 966–931 cm^{-1} typical of NH_3. So we can suppose that the first decomposition step is a release of the two nitrate ions and two $-NH_2$ groups of the histamine molecules with a successive molecular rearrangement; the calculated loss in molecular weight from the TG curves supports this hypothesis.

Experimentally, this first step height increases if the initial sample weight is up to 20–25 mg; this behaviour can be explained by considering the high release of energy in this reaction, which may also involve the $-CH_2-$ of the side chains, when the sample mass is relevant.

The $NiHm_4(NO_3)_2$ complex loses, in the first process, the nitrate and the amino groups of the four

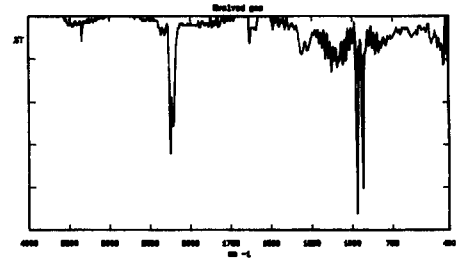

Fig. 8. FTIR spectrum of the TG evolved gas. Resolution: 8 cm^{-1}, 2 scans $°C^{-1}$.

histamine molecules in the same way as the $MeHm_2(NO_3)_2$ complexes, showing the characteristic bands of N_2O and NH_3 in the FTIR spectrum of the evolved gas. The temperatures for the first process of the 1 : 2 and 1 : 4 complexes are similar, while the second process of the 1 : 4 complex is slightly shifted to higher temperature.

The FTIR spectra of the solid state complexes in KBr give useful informations in considering the bands for NH_2, C=N and N–H groups. The standard histamine spectrum shows bands at 3313, 3275 and 3175 cm^{-1}, these are assigned to: stretching vibrations of –NH from the ring and asymmetric and symmetric stretching vibrations from the $-NH_2$ group of the side chain, respectively. These bands are broad, though their maxima are clearly marked. This indicates that $-NH_2$ groups are involved in hydrogen bonds.

On comparing the standard histamine spectrum with the complexes spectra (Fig. 9) a lowering in frequencies may be noted due to the fact that the lone pair of the nitrogen atom is attracted by the metal ion. Therefore, a clearer lowering in frequencies will be seen as the metal bond becomes stronger. This is observed in the NH_2 out of plane bending bands in the zone 900–750 cm^{-1}. Moreover, the shift to higher frequencies in the interval 3400–3000 cm^{-1} for the NH_2 stretching band of the complexes may be explained as a release of hydrogen bonds from the $-NH_2$ groups of the side chains which therefore must be bonded to the metal. This suggests a bidentate binding of histamine. Despite the complexation, the bending frequencies of the C=N-group of the ring do not change even if the metal is bonded to the nitrogen atom, this was also reported for histamine perchlorate complexes and for other benzimidazole complexes [26–30]. We can affirm that the tertiary nitrogen does not take part in the complexation because there are no changes in =N–H frequencies.

Regarding the CoHm and $MeHm_2$ complexes, it has been shown from NMR and IR studies that in aqueous solution the secondary nitrogen atom does not take part in coordination reaction [31,32] and therefore histamine can act as a bidentate ligand.

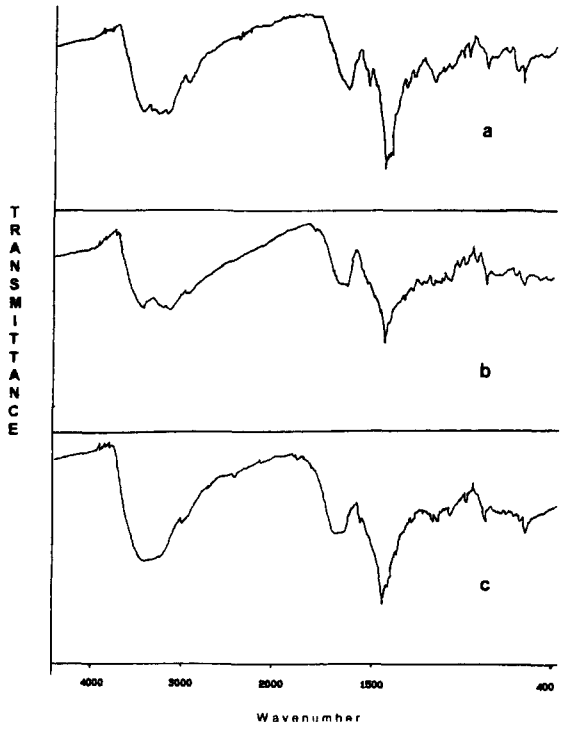

Fig. 9. IR spectra of the solid state complexes: (a) $CoHm_2(NO_3)_2$, (b) $NiHm_2(NO_3)_2$, (c) $CuHm_2(NO_3)_2$. Resolution: 4 cm^{-1}, 20 scans.

3.3. ESCA

For the $Ni^{(II)}$ complexes, $NiHm_2$, $NiHm_2(NO_3)_2$ and $NiHm_4(NO_3)_2$, denominated 1 : 2, 1 : 2-nitrate and 1 : 4-nitrate an ESCA spectroscopy investigation was carried out. In Fig. 10, the N 1*s* spectra of all samples are overlaid and normalised to the same peak height. The peak which falls at 399.8 eV is due to aminic nitrogen (=N–H, $-NH_2$ and C=N–C, indicated as N–H in the figure) while the one at 407 eV accounts for the NO_3^- species (indicated as N–O). The 1 : 2 and 1 : 4 nitrate stoichiometries are confirmed by N–O/N–H

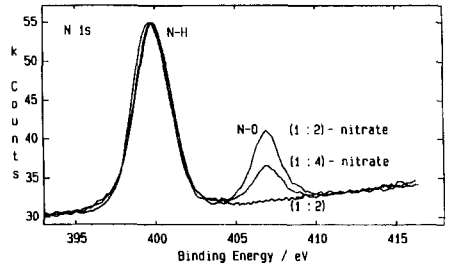

Fig. 10. ESCA spectra from the N 1*s* region for $Ni^{(II)}$ complexes.

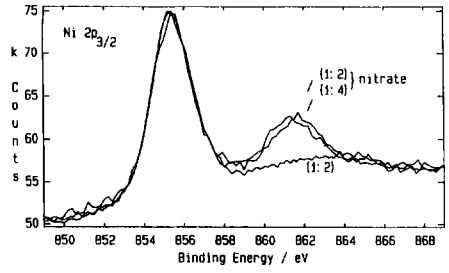

Fig. 11. ESCA spectra from the Ni $2p_{3/2}$ region for $Ni^{(II)}$ complexes.

peak ratios equal to 2 : 1, respectively. For the 1 : 2 complex, only the N–H is present, as expected, and the N/Ni atomic ratio found upon quantification of the peaks is approximately 6 : 1.

The analysis of the Ni $2p$ region (Fig. 11), is even more interesting as the Ni ion coordination can be inferred. The peak position of the Ni $2p_{3/2}$ main transition falls at 855.4 eV corresponding to the doubly ionized Ni cation. In addition to this transition, another peak appears at higher binding energy (about 861 eV). Such transition, known as shake-up satellite, is strongly related to the paramagnetism of the emitting ion [33]. The data show that the 1 : 2-nitrate and 1 : 4-nitrate complexes exhibit shake-up transitions and are paramagnetic, while the 1 : 2 complex is diamagnetic.

Since all known square planar $Ni^{(II)}$ complexes are diamagnetic, we can conclude that the $NiHm_2$ complex has square planar coordination, whereas the nitrate complexes are octahedral.

4. Conclusions

The complexes were synthetized according with published work; sometimes, procedural changes were required in order to precipitate complexes not isolated and characterized before.

The thermoanalytical characterization, improved by the coupled TG–FTIR analysis, completes the few available thermoanalytical data and allows to propose a decomposition mechanism.

ESCA spectroscopy shows to be a useful technique to investigate metal ion coordination and stoichiometries of Ni complexes.

References

[1] A.C. Andrews, T.D. Lyons, T.D. O'Brien, J. Chem. Soc. 84 (1962) 1776.
[2] J.A. Wells, Ann. N.Y. Acad. Sci. 50 (1948) 1202.
[3] W.J. Eibeck, F. Holmes, W.T. Thomas, J. Chem Soc. (1969) 113.
[4] R. Balachandra, A.R. Mathur, J. Inorg. Nucl. Chem. 33 (1971) 809.
[5] B.L. Michel, A.C. Andrews, J. Am. Chem. Soc. 77 (1955) 5291.
[6] A. Chakravorty, F.H. Cotton, J. Phys. Chem. 67 (1963) 2878.
[7] J. Zarembovitch, J. Chim. Phys. 63 (1966) 445.
[8] J. Zarembowitch, J. Chim. Phys. 63 (1966) 420.
[9] F. Holmes, F. Jones, J. Chem. Soc. (1962) 2818.
[10] D.D. Perrin, V.S. Sherma, J. Chem. Soc. A (1968) 446.
[11] B. Rao, H.B. Mathur, J. Inorg. Nucl. Chem. 33 (1971) 809.
[12] G. Weitzel, A.M. Fretzdorff, Z. Physiol. Chem 305 (1956) 1.
[13] J.J. Bonnet, S. Jeannin, Y. Jeannin, S. Rzokiewicz, Compt. Rendu 269 (1969) 1145.
[14] J.J. Bonnet, Y. Jeannin, Bull. Soc. Franc. Mineral. Cristallogr. 95 (1972) 61.
[15] A. Lodzinska, M. Syrocki, Polish J. Chem. 52 (1978) 2305.
[16] G. Weitzel, A. Fretzdorff, Z. Physiol. Chem. 305 (1956) 1.
[17] J.J. Bonnet, J. Jeannin, Acta Cryst. B (1972) 1079.
[18] A. Lodzinska, E. Guzowska, Polish J. Chem. 53 (1979) 1407.
[19] J.J. Bonnet, Y. Jeannin, Bull. Soc. Franc. Mineral. Cristallogr. 93 (1970) 287.
[20] A.B.P. Lever, Inorganic Electronic Spectroscopy, New York, 1968, p. 333.
[21] P. Saarinen, Kem.-Kemi 18 (1991) 412.
[22] D.R. Clark, K.J. Gray, Lab. Pract. 40 (1991) 77.
[23] P.R. Solomon, M.A. Serio, R.M. Carangelo, R. Bassilakis, Z.Z. Yu, S. Charpenay, J. Whelan, J. Anal. Appl. Pyrolysis 19 (1991) 1.
[24] J.H. Scofield, J. Elec. Spectrosc. Relat. Phaenom. 8 (1976) 129.
[25] M.R. Feliz, L. Capparelli, J. Phys. Chem. 88 (1984) 300.
[26] R. Curini, G. D'Ascenzo, G. De Angelis, A. Marino, Thermochim. Acta 99 (1986) 259.
[27] R. Curini, G. D'Ascenzo, S. Materazzi, A. Marino, Thermochim. Acta 200 (1992) 169.
[28] S. Materazzi, G. D'Ascenzo, R. Curini, L. Fava, Thermochim. Acta 228 (1993) 197.
[29] S. Materazzi, R. Curini, G. D'Ascenzo, Thermochim. Acta 286 (1996) 1.
[30] T.J. Lane, I. Nakagawa, J.L. Walter, Inorg. Chem. 1 (1962) 267.
[31] C.C. MacDonald, W.E. Phyllips, J. Am. Chem. Soc. 85 (1963) 3739.
[32] J. Zarembovitch, J. Chem. Phys. 63 (1969) 445.
[33] L.J. Matienzo, L.I. Yin, S.O. Grim, W.E. Swartz Jr., Inorg. Chem. 12 (1973) 2762.